Cell. Mol. Life Sci. (2012) 69:2075–2089
DOI 10.1007/s00018-011-0913-1

Cellular and Molecular Life Sciences

RESEARCH ARTICLE

Neuronal ceroid lipofuscinosis protein CLN3 interacts with motor proteins and modifies location of late endosomal compartments

Kristiina Uusi-Rauva · Aija Kyttälä · Rik van der Kant · Jouni Vesa · Kimmo Tanhuanpää · Jacques Neefjes · Vesa M. Olkkonen · Anu Jalanko

Received: 29 June 2011 / Revised: 8 December 2011 / Accepted: 29 December 2011 / Published online: 20 January 2012

Abstract CLN3 is an endosomal/lysosomal transmembrane protein mutated in classical juvenile onset neuronal ceroid lipofuscinosis, a fatal inherited neurodegenerative lysosomal storage disorder. The function of CLN3 in endosomal/lysosomal events has remained elusive due to poor understanding of its interactions in these compartments. It has previously been shown that the localisation of late endosomal/lysosomal compartments is disturbed in cells expressing the most common disease-associated CLN3 mutant, CLN3Δex7-8 (c.462-677del). We report here that a protracted disease causing mutant, CLN3E295K, affects the properties of late endocytic compartments, since overexpression of the CLN3E295K mutant protein in HeLa cells induced relocalisation of Rab7 and a perinuclear clustering of late endosomes/lysosomes. In addition to the previously reported disturbances in the endocytic pathway, we now show that the anterograde transport of late endosomal/lysosomal compartments is affected in CLN3 deficiency. CLN3 interacted with motor components driving both plus and minus end microtubular trafficking: tubulin, dynactin, dynein and kinesin-2. Most importantly, CLN3 was found to interact directly with active, guanosine-5′-triphosphate (GTP)-bound Rab7 and with the Rab7-interacting lysosomal protein (RILP) that anchors the dynein motor. The data presented in this study provide novel insights into the role of CLN3 in late endosomal/lysosomal membrane transport.

Keywords CLN3 · Motor protein · Neuronal ceroid lipofuscinosis · Rab7 · RILP

Abbreviations

ER	Endoplasmic reticulum
GST	Glutathione S-transferase
GTP	Guanosine-5′-triphosphate
LAMP-1	Lysosomal-associated membrane protein 1
RILP	Rab7-interacting lysosomal protein
SBDS	Shwachmann-Bodian-Diamond syndrome protein
siRNA	Small interfering RNA

Introduction

CLN3 is a highly conserved multipass transmembrane protein present in late endosomes and lysosomes (reviewed in [1]). In neurons, it is additionally localised to early

Electronic supplementary material The online version of this article (doi:10.1007/s00018-011-0913-1) contains supplementary material, which is available to authorized users.

K. Uusi-Rauva · A. Kyttälä · A. Jalanko (✉)
National Institute for Health and Welfare and FIMM, Institute for Molecular Medicine Finland, Biomedicum Helsinki, PO Box 104, 00251 Helsinki, Finland
e-mail: Anu.Jalanko@thl.fi

R. van der Kant · J. Neefjes
Division of Cell Biology, The Netherlands Cancer Institute, 1066 CX Amsterdam, Netherlands

J. Vesa
Department of Human Genetics, David Geffen School of Medicine at UCLA, Gonda Neuroscience and Genetics Research Center, Los Angeles, CA 90095-7088, USA

K. Tanhuanpää
Light Microscopy Unit, Institute of Biotechnology, University of Helsinki, PO Box 56, 00014 Helsinki, Finland

V. M. Olkkonen
Minerva Foundation Institute for Medical Research, Biomedicum Helsinki, 2U, Tukholmankatu 8, 00290 Helsinki, Finland

endosomes, neuronal extensions and synaptosomes [2–5]. CLN3 is mutated in classical juvenile onset neuronal ceroid lipofuscinosis (classical juvenile NCL or juvenile CLN3 disease, earlier referred as JNCL or Batten disease) [6]. Juvenile CLN3 disease is a recessively inherited progressive neurodegenerative disorder characterised by lysosomal accumulation of autofluorescent lipopigment, epileptic seizures, blindness, decline in motor and cognitive skills, and premature death (reviewed in [7]).

The exact function of the CLN3 protein is currently unknown. Based on the phenotypes of CLN3-deficient mammalian cells, alongside yeast and animal models, CLN3 has been proposed to function in multiple cellular processes including autophagy, apoptosis, lipid metabolism, intracellular signalling, RNA metabolism and maintenance of lysosomal/vacuolar size, pH and amino acid homeostasis [8–20].

Protein interaction studies that link CLN3 directly to specific cellular functions support the multifunctional role of CLN3 suggesting that several defective pathways may contribute to the disease mechanism. CLN3 has been shown to interact with calsenilin, a protein mediating calcium-induced cell death [21]. An interaction between Btn1p and Sdo1p, *Saccharomyces cerevisiae* orthologues of CLN3 and Shwachmann-Bodian-Diamond syndrome protein (SBDS), respectively, was suggested to regulate yeast vacuolar homeostasis through a ribosome maturation pathway [22]. Recently, loss of the novel CLN3-myosin-IIB interaction was proposed to result in cell migration defects of Cln3-deficient mouse fibroblasts [23].

CLN3 has frequently been associated with intracellular membrane trafficking and defects in these functions may contribute to the onset of CLN3 disease. Trafficking abnormalities in several intracellular compartments have been reported to be due to deficiency of CLN3 or its *Schizosaccharomyces pombe* orthologue, Btn1p. These include impaired Golgi protein sorting [24] and exit of mannose 6-phosphate receptor from the *trans*-Golgi network [25], defects in endocytosis [3, 26, 27] and in the fast axonal transport of optic nerves [28]. Additionally, aberrant processing and delivery of lysosomal cathepsins has been suggested to result from CLN3 deficiency [3, 13, 25]. Furthermore, the cytoskeleton was one of the three major pathways affected in gene expression profiling of *Cln3* knock-out mouse primary neurons, with subunit p25 of the dynactin complex being the most down-regulated component [29]. CLN3 has been shown to interact with the cytoskeletal fodrin and multifunctional Na^+, K^+ ATPase, both implicated in endocytic events ([26] and references therein, [30]). Moreover, we have reported that CLN3 interacts with the endocytic microtubule-binding protein Hook1 and that high expression levels of CLN3 induce aggregation of the Hook1 protein, potentially through dissociation from microtubules [27]. The finding that Hook1 interacts with several mammalian endocytic Rab GTPases, including Rab7 which controls late endosomal transport, suggests a functional connection between CLN3 and the Rab proteins [27].

In this study, we analysed the role of mammalian CLN3 in late endosomal/lysosomal membrane trafficking. We report that CLN3 interacts with both retro- and anterograde microtubular motor complexes responsible for the movement of late endosomes and lysosomes: the Rab7/RILP/dynein/dynactin complex for minus end-directed transport, and the kinesin-2 complex for plus end-directed transport. Further experiments suggest that CLN3 is involved in the intracellular localisation and motility of late endosomal/lysosomal compartments.

Materials and methods

cDNA constructs

The following constructs used in this study have been described earlier; CLN3-pCMV5, CLN3E295K-pCMV5, CLN3 1–33 -pGEX4T-3 (GST-CLN3 1–33), CLN3 232–280 -pGEX4T-1 (glutathione S-transferase [GST]-CLN3 232–280), Rab7-pCDNA4/HisMaxC (Xpress-Rab7), Rab7-pEGFP-C, Rab7Q67L-pET28a (His_6-Rab7Q67L), Rab7wt-pVP16, Rab7T22N-pVP16, Rab7Q67L-pVP16, RILP-pETM-11 (His_6-RILP) and $p50^{dynamitin}$-pEGFP-C [2, 27, 31–34]. The mammalian two-hybrid vectors pM and pVP16 and the reporter vector pG5CAT were obtained from Clontech (Palo Alto, CA, USA). For the generation of the CLN3 mammalian two hybrid expression vectors, two PCR-amplified CLN3 cDNA regions encoding the cytoplasmic N-terminal peptide 1–40 and the major cytolasmic loop peptide 232–273 were cloned separately into the pGEM-T Easy vector (Promega, Madison, WI, USA) from which they were subcloned into the pM vector in frame with the GAL4 DNA-binding domain. Human (HeLa) cell open reading frame of RILP cDNA (NM_031430.2) was inserted into the EcoRI site of pCDNA4/HisMaxC (Invitrogen, Carlsbad, CA, USA) to generate the expression vector for the N-terminally Xpress-tagged RILP fusion protein.

Antibodies

Preparation of rabbit polyclonal antibodies against RILP, CLN3 amino acids 1–33 and amino acids 242–258 has been described earlier [4, 31, 35]. The mouse monoclonal antibody (H4A3) against human lysosomal-associated membrane protein 1 (LAMP-1), which was developed by J. Thomas August and James E.K. Hildreth, was obtained from the Developmental Studies of Hybridoma Bank

developed under the auspices of the NICHD and maintained by The University of Iowa, Iowa City, IA, USA. Mouse monoclonal anti-Xpress was purchased from Invitrogen. Mouse monoclonal antibodies against EEA1, KIF3A and $p150^{Glued}$ were obtained from BD Biosciences (San Jose, CA, USA). Mouse monoclonal antibodies against β-tubulin, dynein intermediate chain and Rab7 were from Sigma (St. Louis, MO, USA). Secondary polyclonal antibodies used in western blotting were swine anti-rabbit immunoglobulins/HRP and goat anti-mouse immunoglobulins/HRP (Dako, Glostrup, Denmark). Secondary antibodies used in immunofluorescence stainings were Texas Red AffiniPure Donkey Anti-Rabbit IgG (H+L), Cy5-conjugated Affinipure $F(ab')_2$ Fragment Goat Anti-Mouse IgG (H+L) and Fluorescein (FITC) AffiniPure Donkey Anti-Mouse IgG (H+L) (Jackson ImmunoResearch Laboratories, West Grove, PA, USA).

Confocal immunofluorescence microscopy and image analysis

HeLa cells grown on coverslips were transfected with FuGENE 6 or FuGENE HD Transfection reagent (Roche Applied Science, Mannheim, Germany) according to the manufacturer's instructions. Where specified, 48 h after transfection, cells were treated with 33 μM nocodazole for 1 h followed by fixation. Cells were fixed either with ice-cold methanol for 7 min at −20°C followed by blocking with 0.5% BSA in PBS for 30 min or with 4% paraformaldehyde in PBS for 15 min at room temperature, followed by permeabilisation and blocking with 0.2% saponine, 0.5% BSA in PBS. Primary and secondary antibodies were diluted in the blocking buffer, and each separately incubated for a minimum of 1 h at room temperature. Cells were then washed and mounted with FLUORO GEL mounting medium (Electron Microscopy Sciences, Hatfield, PA, USA). The specimens were viewed with a Leica TCS SP1 laser scanning confocal microscope. The acquisition software used was Leica LCS software. In co-localisation analyses, Pearson's correlation value was calculated for each outlined cell with the co-localisation tool of Image-Pro Plus 7.0 (Bethesda, MD, USA). Student's *t* test was used for statistical analysis. For illustration, images were processed with Adobe Photoshop 8.0 and Adobe Illustrator 11.0.0 software.

CLN3 RNA interference

CLN3 small interfering RNAs (siRNAs) were designed to target sequences GUGGGAUUUGUGCUGCUGGAA and CCAGCCUCUCCCUUCGGGAAA of exons 6 and 10, respectively (Sigma-Proligo, The Woodlands, TX, USA). siCONTROL Non-targeting siRNA #1 (Dharmacon, Lafayette, CO, USA) was used as a control siRNA to monitor possible off-target effects. Samples of 3.5×10^4 HeLa cells were plated on coverslips in a 6-well culture dish, incubated overnight and transfected twice at 48-h intervals either with 40 pmol of each CLN3 siRNA or 80 pmol of control siRNA and 2 μl Lipofectamine 2000 reagent (Invitrogen). Transfection efficiency was verified to be 100% by BLOCK-iT Fluorescent Oligo control siRNA transfection (Invitrogen). Efficiency of *CLN3* silencing was analysed by quantitative polymerase chain reaction (qPCR) because the available antibodies do not recognise the endogenous CLN3 protein. For these purposes, RNA from control and CLN3 siRNA-transfected cells was extracted using Qiagen RNeasy kit, and 1 μg of total RNA was subsequently reverse transcribed into complementary DNA (cDNA) using TaqMan Reverse Transcription Reagents kit (Applied Biosystems/Roche). Quantity of CLN3 and housekeeping cDNAs were analysed in triplicates using Power SYBR Green PCR Master Mix kit (Applied Biosystems/Life Sciences), 10 ng of total cDNA as a template and CLN3 or housekeeping peptidylprolyl isomerase A (PPIA) primers. Data obtained from quantitative real-time PCR by ABI PRISM 7000 sequence detection system (Applied Biosystems) was analysed using the comparative CT method ($2^{\Delta\Delta CT}$). In CLN3 siRNA-transfected cells, the mean relative *CLN3* mRNA expression was 44% as compared to that in control siRNA-transfected cells.

Cytoplasmic acidification

Cytoplasmic acidification, developed by Heuser [36], was performed as described [37]. Briefly, HeLa cells transfected either with CLN3 siRNA or control siRNA oligos were washed three times with Hepes-buffered Ringer's solution pH 7.2 (155 mM NaCl, 5 mM KCl, 2 mM $CaCl_2$, 1 mM $MgCl_2$, 2 mM NaH_2PO_4, 10 mM Hepes pH 7.2, 10 mM glucose, 0.5 mg/ml BSA) at 37°C over 15 min followed by further incubation in the same buffer or in Hepes-buffered Ringer's solution pH 6.9 (80 mM NaCl, 70 mM Na acetate, 5 mM KCl, 2 mM Ca Cl_2, 1 mM $MgCl_2$, 2 mM NaH_2PO_4, 10 mM Hepes pH 6.9, 10 mM glucose, 0.5 mg/ml BSA) for 1 h at 37°C. Cells were then fixed immediately with 4% paraformaldehyde in PBS and stained for immunofluorescence microscopy with LAMP-1 antibody. In microscopy analysis, cells were classified in one of three phenotypic categories described in "Results" based on the pattern of LAMP-1 immunofluorescence signal. The analysis was done single-blindly.

Co-immunoprecipitation

Co-immunoprecipitations were performed as described [26] with minor modifications. Briefly, COS-1 cells plated on a 10-cm culture dish and incubated overnight were

transiently transfected with FuGENE 6 or FuGENE HD Transfection reagent (Roche) according to manufacturer's instructions. After 48 h, cells were lysed in 800 µl of ice-cold lysis buffer (10 mM Hepes pH 7.4, 150 mM NaCl, 0.5 mM $MgCl_2$, 10% glycerol, 0.5% Triton X-100, Complete Protease Inhibitor Cocktail) followed by centrifugation to remove nuclear debris. Half of the lysate was used for one immunoprecipitation, diluted to 1 ml with lysis buffer and pre-cleared with 14% heat-killed and formalin-fixed *Staphylococcus aureus* cells (standardised PANSORBIN® Cells, Calbiochem; Merck, Darmstadt, Germany). Pre-cleared samples were then incubated with or without (matrix control) antibody at +4°C overnight, followed by further incubation with *S. aureus* for 2 h. Immobilised protein complexes were washed with lysis buffer, re-suspended in Laemmli buffer and analysed by western blotting with antibody against proteins of interest. Cells untransfected for CLN3 (untransfected cell control) were used to exclude the possible unspecific binding properties of CLN3 antibodies.

Mammalian two-hybrid assay

COS-1 cells (900,000) were plated on a 10-cm culture dish, incubated overnight and transiently transfected with 2.7 µg of each hybrid vector (GAL4 DNA-binding domain vector pM and DNA-activation domain vector pVP16) and 0.54 µg of reporter vector (pG5CAT) combined with 18 µl of FuGENE 6 Transfection reagent (Roche). After 48 h, cells were lysed in 1 ml of lysis buffer included in the CAT ELISA kit (Roche). Protein concentration was determined by Bio-Rad DC Protein Assay (Bio-Rad Laboratories). To verify similar protein expression levels in the samples, equal amounts of total protein were analysed by western blotting with Rab7, CLN3 1–33 and CLN3 242–258 antibodies. Next, 50 µg of total protein diluted to a concentration of 250 µg/ml were analysed for CAT expression by the CAT ELISA according to manufacturer's instructions. Each sample was analysed in triplicates in the CAT ELISA and the average was considered as the equivalent to the amount of CAT in the sample. Untransfected cells and co-transfection of empty vectors were used to monitor background and basal CAT expression, respectively. In addition, each CLN3 and Rab7 recombinant vector was co-transfected separately with an empty two-hybrid counterpart vector to monitor possible autoactivity. Due to variation in the general expression levels of the CAT reporter gene, the results of each individual experiment were normalised with the averaged CAT expression in the corresponding sample series. Normalised values from independent experiments were combined and the Student's *t* test was used for statistical analysis.

GST-CLN3 pull-down of purified His_6-Rab7Q67L and His_6-RILP

GST, GST-CLN3 1–33 and GST-CLN3 232–280 were produced in *Escherichia coli* and purified by coupling 100 µg fusion proteins to Glutathione Sepharose 4B beads (GE Healthcare, Sweden) overnight at +4°C. After washing, the beads were used for pull-down of purified His_6-Rab7Q67L (20 µg) and/or His_6-RILP (10 µg) as previously described [34], with minor modifications. The His_6-tagged recombinant proteins were incubated with Sepharose-bound GST proteins overnight at +4°C, and after intensive washing, the protein complexes were eluted by Laemmli sample buffer.

Fluorescence Recovery after Photobleaching (FRAP)

FRAP experiments were performed with a Leica TCS SP5 confocal microscope at 37°C under 5% CO2 using a 63x NA 0.9 dipping water objective and 280mW OPSL laser. A 42-μm^2 area, containing EGFP-Rab7 endosome/lysosome clusters, was bleached with one scan with 70% power from the laser at 488nm. Fluorescence recovery was followed for 500 s and the intensity data were exported to Microsoft Excel and corrected for bleaching of the control area from the same cell during recovery.

Results

The CLN3E295K mutant clusters Rab7 and late endosomes/lysosomes in a perinuclear region

Previous studies with mammalian cell models of juvenile CLN3 disease have shown that mouse cerebellar precursor cells expressing the endoplasmic reticulum (ER)-retained CLN3Δex7-8 (c.462-677del) mutant protein display changes in steady-state localisation of endosomal compartments [3]. To obtain more information on the role of CLN3 in membrane trafficking, we utilised another CLN3 mutant, the protracted disease causing late endosome/lysosome-localised CLN3E295K mutant [38], and analysed the effect of high expression levels of this mutant on localisation of EEA1-positive early endosomes, LAMP-1-positive late endosomes/lysosomes and EGFP-Rab7 in HeLa cells by immunofluorescence microscopy. The distribution of CLN3E295K differed from wild-type CLN3. The CLN3E295K mutant located to vesicles clustered in a perinuclear region (Fig. 1d, g) while the vesicles containing wild-type CLN3 were more dispersed (Fig. 1a). As expected, both CLN3 and the CLN3E295K mutant located to LAMP-1-positive late endosomes and lysosomes (Fig. 1c, f) indicating that the mutant protein was not mistargeted but, instead, the distribution of LAMP-1-positive

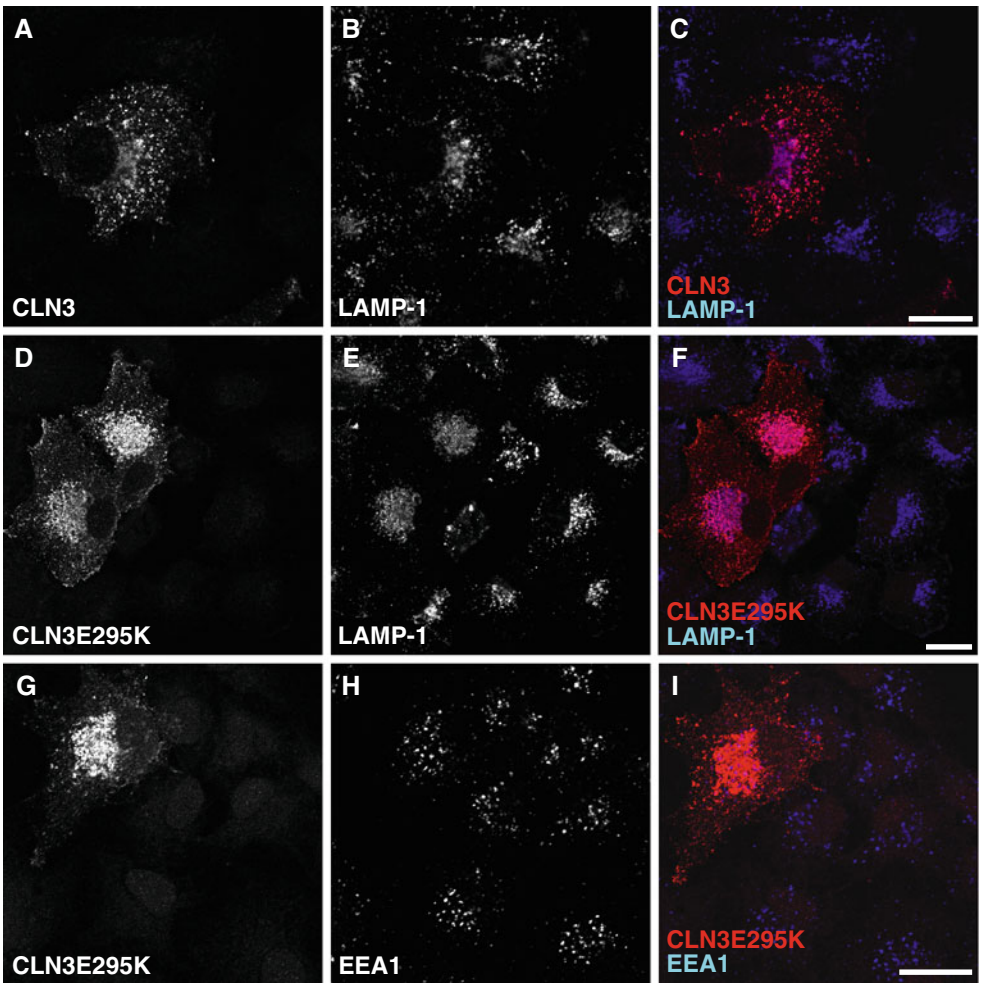

Fig. 1 **a–i** The CLN3E295K mutant clusters late endosomes/lysosomes in a perinuclear region. Wild-type CLN3 (**a**) and the CLN3E295K mutant (**d**, **g**) were separately expressed in HeLa cells and analysed with endosomal/lysosomal markers by immunofluorescence microscopy. Contrary to the cells expressing wild-type CLN3 (**b**), expression of CLN3E295K induced a perinuclear clustering of LAMP-1-positive late endosomes and lysosomes (**e**), with no obvious effect on early endosomal EEA1-positive compartments (**h**). **c**, **f** and **i** represent the overlays of the immunofluorescence signals of indicated proteins. *Scale bars* 20 μm

late endosomal/lysosomal compartments was affected by the overexpression of CLN3E295K mutant (Fig. 1e). Analysis of EEA1-positive compartments showed that CLN3E295K had no detectable effect on the steady-state distribution of early endosomes (Fig. 1h). Notably, a detailed analysis of the distribution of EGFP-Rab7 on LAMP-1-positive late endosomes and lysosomes suggested that the association of EGFP-Rab7 on these vesicles was also affected by the CLN3E295K mutant (Fig. 2). Compared to EGFP-Rab7, expressed alone (Fig. 2c, c′) or together with wild-type CLN3 (Fig. 2g, g′, h, h′), EGFP-Rab7, expressed together with CLN3E295K in HeLa cells (Fig. 2l, l′, m, m′) appeared to be more concentrated on CLN3 and LAMP-1-positive compartments. This was verified by quantification of co-localisation between CLN3 and EGFP-Rab7 and between EGFP-Rab7 and LAMP-1 (Fig. 3). In CLN3E295K/EGFP-Rab7-expressing cells, co-localisation between CLN3 and EGFP-Rab7 and between EGFP-Rab7 and LAMP-1 was increased approximately by 20% compared to that in CLN3/EGFP-Rab7 or EGFP-Rab7-transfected cells (Fig. 3). This data suggests that CLN3 contributes to the steady-state localisation of lysosomes and interestingly, compartmentalisation of Rab7.

CLN3E295K-induced perinuclear clustering of late endosomes/lysosomes requires intact microtubules and dynactin complex

Next, we investigated if the CLN3E295K-induced clustering of LAMP-1-positive compartments is dependent on microtubular trafficking. We treated CLN3E295K-transfected HeLa cells with the microtubule-depolymerizing agent nocodazole, which resulted in dispersion of CLN3E295K and LAMP-1-positive compartments throughout the cytoplasm

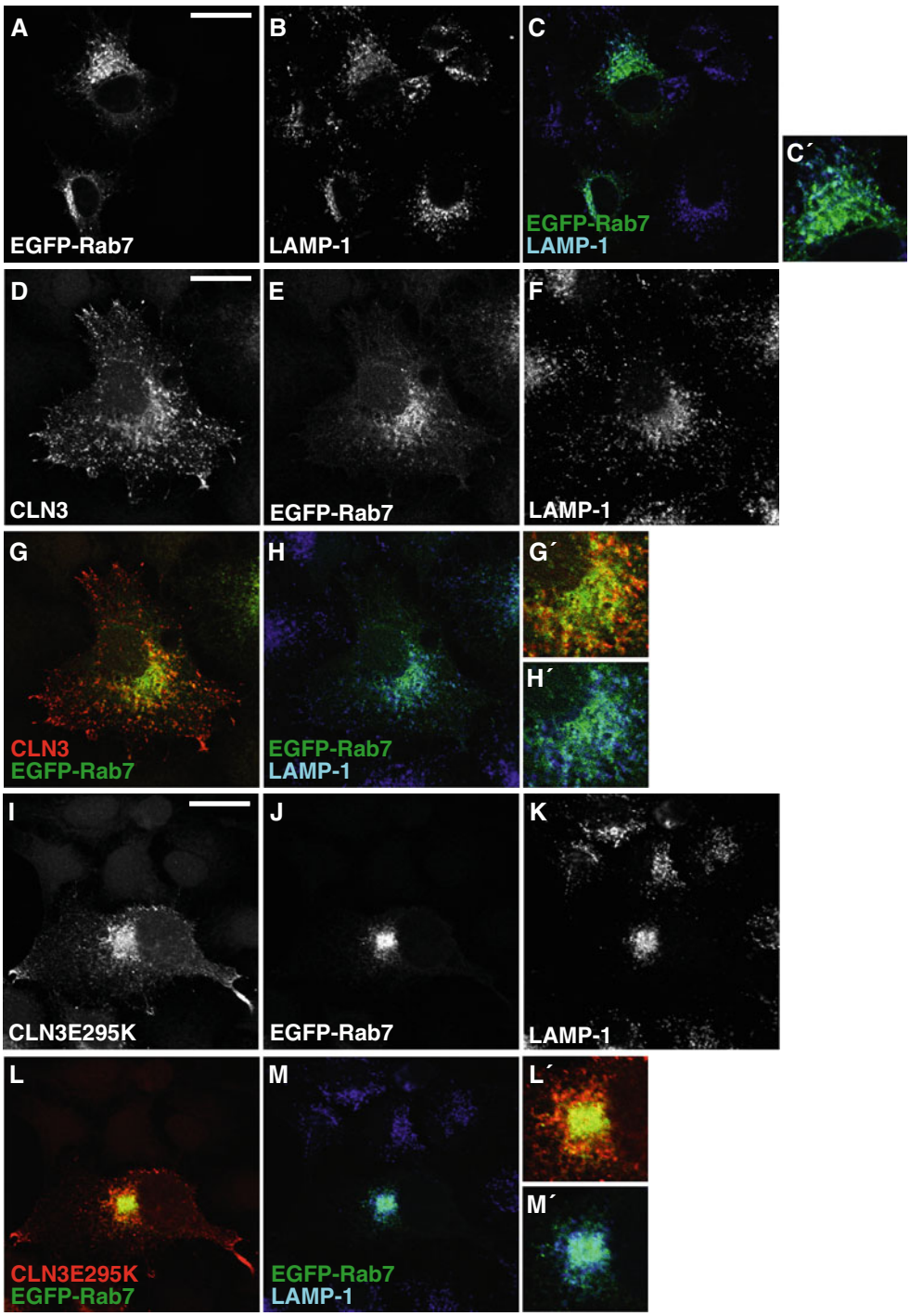

Fig. 2 **a–m** CLN3E295K affects compartmentalisation of EGFP-Rab7. HeLa cells transfected with EGFP-tagged Rab7 alone (**a–c**) or together with either wild-type CLN3 (**d–h**) or the CLN3E295K mutant (**i–m**) were processed for CLN3, CLN3E295K, EGFP-Rab7 and LAMP-1 immunofluorescence microscopy. Compared to the other conditions, EGFP-Rab7 in the CLN3E295K-transfected cells appeared to be more concentrated on CLN3E295K (**l**) and LAMP-1-positive (**m**) compartments. **c′**, **g′**, **h′**, **l′** and **m′** represent magnifications of co-localisation area in the corresponding images. *Scale bars* 20 μm

(Fig. 4). Also, when the dynein/dynactin complex was disrupted by over-expressing the dynactin subunit $p50^{dynamitin}$ [39], CLN3E295K and LAMP-1-positive compartments were again dispersed into the cytoplasm (Fig. 4). These results suggest that the CLN3E295K-induced perinuclear clustering of late endosomes/lysosomes is dependent on intact microtubules and a functional dynactin complex, the essential components of microtubular transport.

CLN3 is required for the outward movement of late endosomes/lysosomes

Changes in the steady-state localisation of late endosomal compartments may result from disturbances in the movement of endocytic organelles. It has already been reported that the trafficking of endocytosed material to the late endocytic compartments is impaired in CLN3-deficient

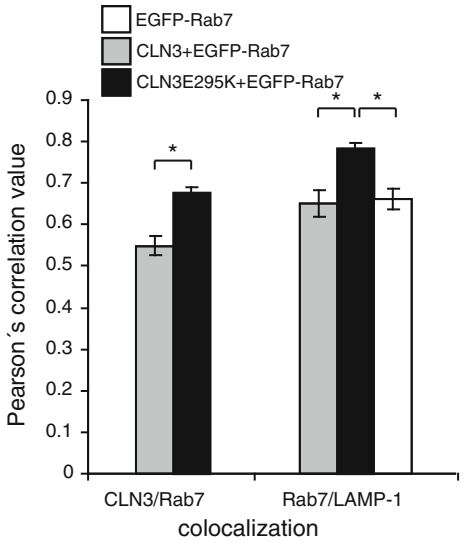

Fig. 3 Quantification of the co-localisation between CLN3 and EGFP-Rab7, and EGFP-Rab7 and LAMP-1. To quantify the results visualised in Fig. 2, immunofluorescence images of HeLa cells tranfected for EGFP-Rab7 alone, CLN3 and EGFP-Rab7, or CLN3E295K and EGFP-Rab7 were analysed by measuring Pearson's correlation value for co-localisation between indicated immunofluorescence stainings. Each data point represents mean ± SEM of 15 cells of one experiment. $*P < 0.0005$ (one-tailed Student's *t* test)

cells [3, 27]. Here, we tested whether CLN3 also contributes to the anterograde transport of late endosomes and lysosomes.

Cytoplasmic acidification has been reported to relocate late endosomes and lysosomes from the cell center to the periphery [36], and has been used to analyse kinesin-mediated organelle transport [37, 40, 41]. We applied this to analyse anterograde movement of LAMP-1-positive late endosomes and lysosomes in HeLa cells transfected with non-targeting control siRNA or siRNA for a specific knock-down of CLN3. Transfected cells were treated with Ringer's solution pH 7.2, or with Ringer's solution pH 6.9, for cytoplasmic acidification, fixed and stained for immunofluorescence microcopy analyses. Cells were classified in three phenotypic categories based on the intracellular localisation of LAMP-1-positive compartments as deduced by immunofluorescence microscopy (Fig. 5a): accumulation of LAMP-1-positive compartments in a perinuclear region with some cytoplasmic vesicles (normal), loose peripheral clusters (dispersed) and tight peripheral clusters (extremely dispersed). The analysis showed that late endosomes and lysosomes were already dispersed in most of the control cells treated with Ringer's pH 7.2, while localisation was unaffected in approximately 16% of cells (Fig. 5b). Incubation of cells in a more acidic solution (pH 6.9) resulted in an increased percentage of cells with tight peripheral clusters, as expected (Fig. 5b). However, the response of cells transfected with CLN3 siRNAs to the cytoplasmic acidification was different from that of control cells. While the control cells treated with Ringer's pH 7.2 showed 18% of extremely

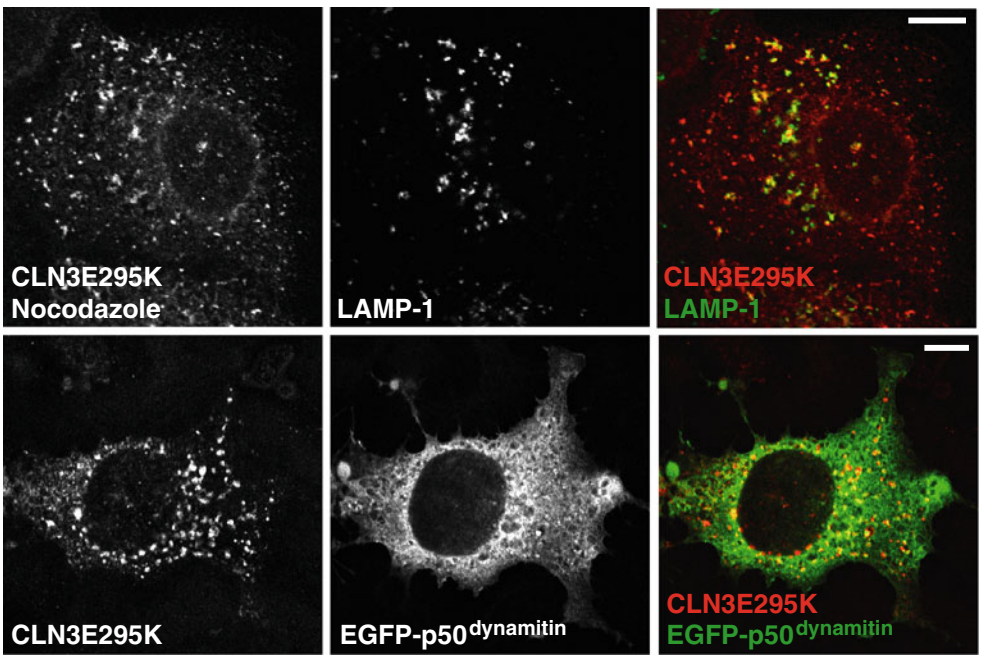

Fig. 4 The CLN3E295K-induced perinuclear clustering of lysosomes is dependent on intact microtubules and functional dynactin complex. HeLa cells expressing CLN3E295K were either treated with nocodazole (*upper panel*) or co-expressed with EGFP-p50^{dynamitin} (*lower panel*) and processed for CLN3 and LAMP-1 immunofluorescence microscopy. In both cases, CLN3E295K and LAMP-1-positive perinuclear clusters were lost and instead, corresponding compartments were dispersed throughout the cytoplasm. *Scale bars* 10 μm

dispersed LAMP-1 positive compartments, the corresponding count of CLN3 siRNA-transfected cells was only 6%. The difference was also notable in the cells treated with Ringer's pH 6.9 solution, since CLN3-silenced cell culture showed significantly fewer cells with extremely dispersed late endosomes/lysosomes compared to the control culture (41 vs. 69%) (Fig. 5b). The impaired response of CLN3 siRNA-treated HeLa cells to cytoplasmic acidification suggests that CLN3 also plays an important role in the outward movement of late endosomes and lysosomes.

CLN3 interacts with both minus and plus end-directed microtubular motor protein components

As CLN3 affects late endosomal/lysosomal distribution, it may interact with, and thus influence the function of, minus and/or plus-end motor proteins, dynein/dynactin and kinesin-2, active on late endosomes/lysosomes [37, 42]. This hypothesis was tested by co-immunoprecipitation experiments. CLN3 expressed in COS-1 cells was immunoprecipitated with rabbit polyclonal antibody produced against the major cytoplasmic loop of CLN3 (amino acids 242–258) followed by western blot analysis of endogenous proteins associated to immunoprecipitated CLN3. Interestingly, β-tubulin, the p150^{Glued} of the dynactin complex, dynein intermediate chain (DIC) and KIF3A subunit of the heterotrimeric kinesin-2 complex, were found to interact with CLN3 as they all co-immunoprecipitated with over-expressed CLN3. These proteins were not detected in either of the two controls, the matrix control (devoid of precipitating antibody) and anti-CLN3 immunoprecipitates from untransfected cells (of note, the anti-CLN3 242–258 antibody does not immunoprecipitate endogenous CLN3 protein) (Fig. 6). Together with the data obtained by the cytoplasmic acidification assay, these results suggest that CLN3 may play a role in both minus and plus end-directed microtubule-dependent trafficking.

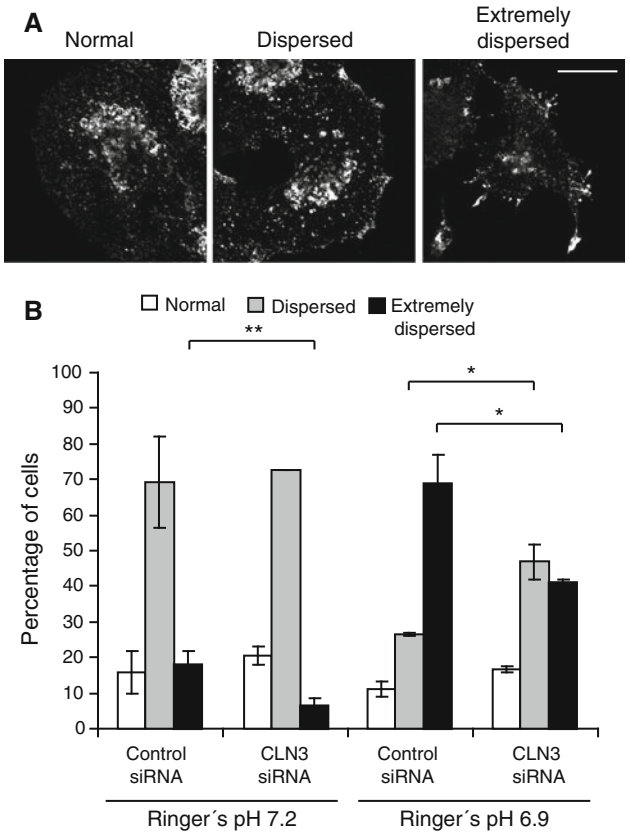

Fig. 5 **a**, **b** Cytoplasmic acidification-driven outward movement of LAMP-1-positive late endosomes and lysosomes is defective in CLN3-silenced HeLa cells. CLN3 siRNA and control siRNA-transfected Hela cells were treated with Ringer's solution pH 7.2 or with Ringer's solution pH 6.9 and processed for LAMP-1 immunofluorescence microscopy. **a** Each analysed cell was classified in one of the three phenotypic categories based on the distribution of LAMP-1 immunofluorescence staining; normal, dispersed and extremely dispersed. **b** The percentage of each phenotype per condition is indicated. Microscopy analyses were carried single-blindly. Each data point represents mean ± SEM of two individual experiments, and at least 150 cells were scored for each condition in each experiment. $*P < 0.04$, $**P = 0.066$ (one-tailed Student's *t* test). *Scale bar* 20 μm

CLN3 interacts with Rab7 and Rab7 effector RILP

We have previously shown that the endocytic Hook1 protein interacts with both CLN3 and the GTPase Rab7, but could not determine whether CLN3 interacted with Rab7 [27]. Considering the role of Rab7 in late endosomal

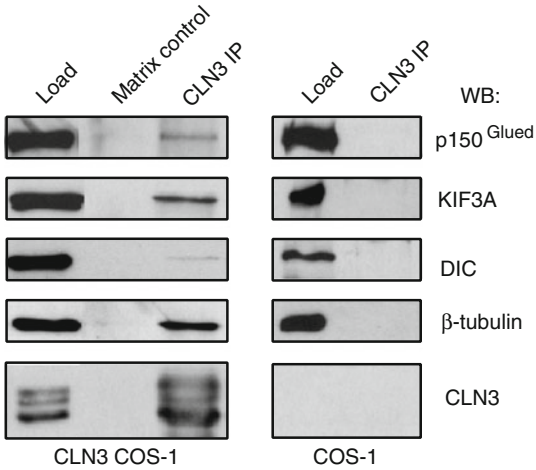

Fig. 6 CLN3 interacts with both minus and plus end-directed motor protein components. COS-1 cells transfected with or without CLN3 (untransfected cell control) were processed for immunoprecipitation with anti-CLN3 242–258 followed by western blotting analysis with antibodies against components of microtubular motor complexes: *β-tubulin* (55 kDa), *p150^{Glued}* (150 kDa), dynein intermediate chain (*DIC*, 74 kDa) and *KIF3A* subunit of the heterotrimeric kinesin-2 complex (80/85 kDa). All tested proteins co-immunoprecipitated specifically with CLN3 (43 kDa). Matrix control represents sample devoid of precipitating antibody. *Load* represents 2% of total protein present in immunoprecipitation

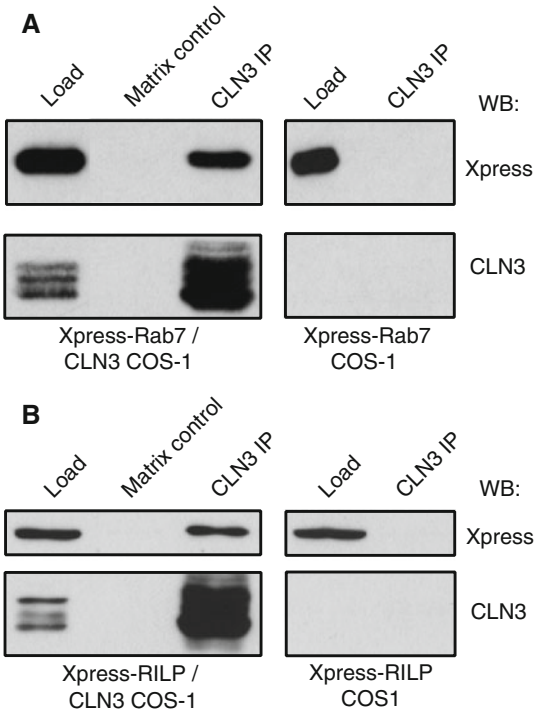

Fig. 7 **a**, **b** *Xpress-Rab7* and *Xpress-RILP* co-immunoprecipitate with CLN3. COS-1 cells transfected for Xpress-tagged Rab7 (**a**) or Xpress-tagged RILP (**b**) with or without CLN3 were processed for immunoprecipitation with anti-CLN3 242–258 followed by western blotting with anti-Xpress and anti-CLN3. Both Xpress-Rab7 (~30 kDa) (**a**) and Xpress-RILP (~60 kDa) (**b**) co-immunoprecipitated only from the cells that also expressed CLN3 (43 kDa). Matrix control represents sample devoid of precipitating antibody. *Load* represents 2% of total protein present in immunoprecipitation

trafficking, the observed changes in the localisation of late endosomes and Rab7 in CLN3 mutant cells, in addition to the novel interactions of CLN3 with microtubular motor proteins, we tested again the possible interaction between CLN3 and Rab7. Here, we co-expressed CLN3 and N-terminally Xpress-tagged Rab7 in COS-1 cells and co-immunoprecipitated CLN3 protein complexes with anti-CLN3 242–258. The presence of Xpress-Rab7 in the CLN3 co-immunoprecipitate was analysed by western blotting with Xpress antibody. Xpress-Rab7 was found to co-immunoprecipitate specifically with CLN3 (Fig. 7a) suggesting that mammalian CLN3 and Rab7 do indeed interact, and therefore may act in concert in mediating endosomal/lysosomal membrane trafficking functions.

It has been previously reported that active, GTP-bound Rab7 forms a complex with Rab7-interacting lysosomal protein (RILP) and oxysterol-binding protein-related 1L (ORP1L) which facilitates the recruitment of the dynein/dynactin complex to late endosomes/lysosomes [34, 35, 43–45]. Since CLN3 was also found to interact with Rab7, we analysed its possible association with RILP. N-terminally Xpress-tagged RILP was expressed with or without CLN3 in COS-1 cells and the cell lysates were processed for CLN3 immunoprecipitation with CLN3 242–258 antibody. Western blotting with Xpress antibody confirmed co-immunoprecipitation of Xpress-tagged RILP with CLN3, indicating that the detected CLN3 interaction with Rab7 may be mediated or accompanied by RILP (Fig. 7b).

Two different cytoplasmic domains of CLN3 interact directly with active, GTP-bound Rab7 and the effector RILP

To determine the Rab7-interacting domain(s) of CLN3, and the preferred nucleotide-bound form of Rab7 participating in the interaction, we utilised a mammalian two-hybrid assay. The cytoplasmic N-terminus (amino acids 1–40) and the major cytoplasmic loop of CLN3 (amino acids 232–273) were separately cloned into the GAL4 DNA-binding domain vector pM. The cytoplasmic C-terminus of CLN3 was excluded from the analysis due to its autonomous transcriptional activation properties observed in previous studies [46] and in our experiments (data not shown). A wild-type Rab7, a GTPase-deficient constitutively active Rab7Q67L mutant and a dominant-negative Rab7T22N mutant, incapable of dissociating GDP, were cloned into the activation domain vector pVP16. Hybrid vectors were then co-expressed in COS-1 cells and putative interactions were analysed by measuring the expression of GAL4-dependent CAT reporter gene by CAT ELISA assay. Three separate assays demonstrated that only the co-expression of CLN3 1–40/Rab7wt and CLN3 1–40/Rab7Q67L resulted in higher CAT expression than the controls (Fig. 8a). This suggests that the binding of the active GTP-bound form of Rab7 is favoured and that the interaction occurs via the N-terminal domain of CLN3.

To test whether CLN3 interacts directly with GTP-bound Rab7 or via interaction with RILP, we employed GST pull-down experiments with purified proteins. GST (control) or the N-terminally GST-tagged CLN3 domains, the N-terminus (amino acids 1–33) or the major cytoplasmic loop (amino acids 232–280), bound to the glutathione Sepharose were incubated with purified His_6-Rab7Q67L and/or His_6-RILP recombinant proteins. The western blot analysis with Rab7 and RILP-specific antibodies revealed a relatively weak but experimentally consistent binding between His_6-Rab7Q67L and the N-terminal domain of CLN3 (Fig. 8b). This suggests a direct interaction between the two proteins. His_6-tagged RILP was only efficiently pulled down by the cytoplasmic loop of CLN3 (Fig. 8b).

The observation that Rab7 and RILP proteins bind different cytoplasmic domains of CLN3 was further supported by the co-immunoprecipitation experiments utilising CLN3 antibody produced against the Rab7 interacting domain of CLN3. CLN3 1–33 antibody co-immunoprecipitated

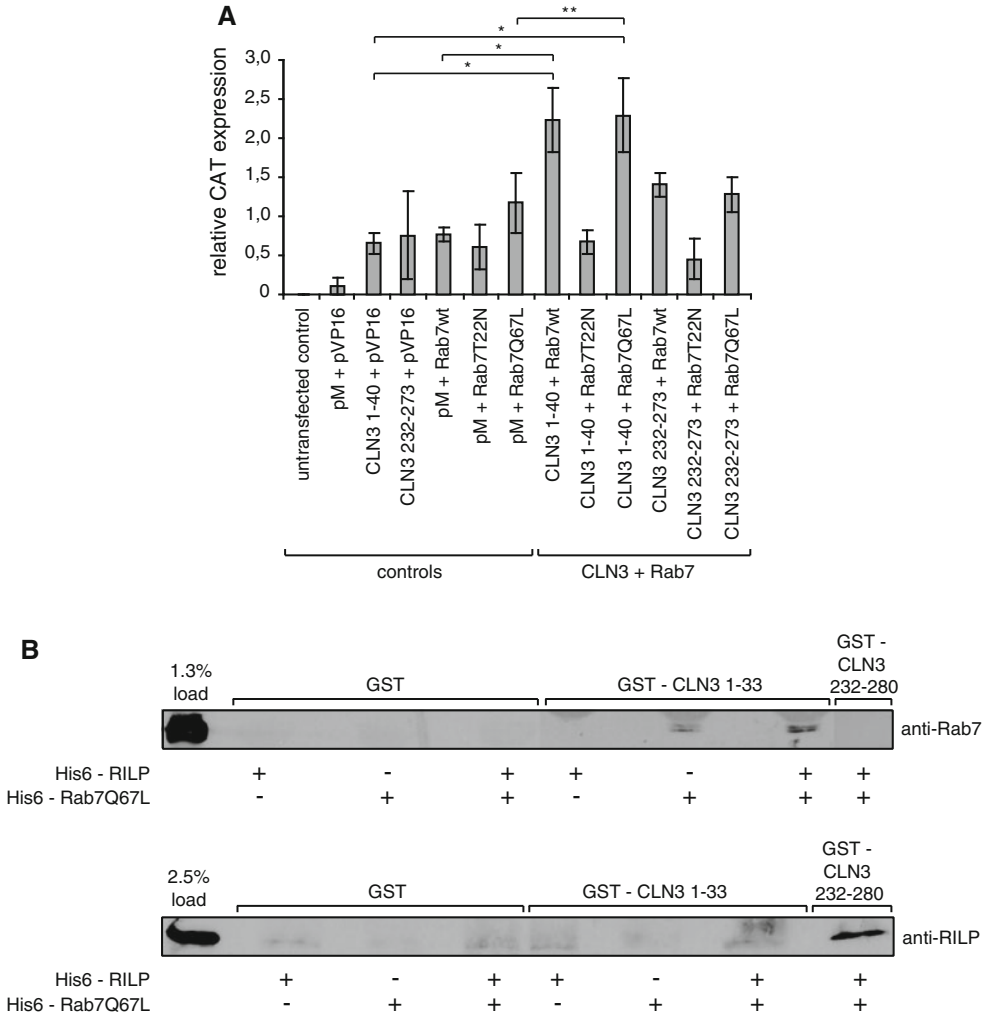

Fig. 8 **a**, **b** CLN3 interacts directly with active, GTP-bound Rab7 and RILP via different cytoplasmic domains. **a** Mammalian two-hybrid experiment with two cytoplasmic CLN3 domains and different nucleotide-bound forms of Rab7, a wild-type Rab7, a GTPase-deficient constitutively active Rab7Q67L mutant, and a dominant-negative Rab7T22N mutant. Only CLN3 1–40/Rab7wt and 1–40/Rab7Q67L two-hybrids resulted in higher CAT expression than the corresponding controls. Each data point represents mean of normalised expression levels of CAT reporter gene of three individual experiments ±sem (one experiment contained CLN3 + Rab7 hybrids only). $*P < 0.05$ and $**P = 0.11$ (one-tailed Student's *t* test). **b** GST (control) or GST-tagged domains of CLN3, the N-terminus (amino acids 1–33) and cytoplasmic loop (232–280) purified by coupling to glutathione Sepharose were incubated with purified His_6-tagged Rab7Q67L and/or RILP recombinant proteins. Figure shows the results of the subsequent western blot analyses with Rab7 and RILP specific antibodies. His_6-Rab7Q67L (~23 kDa) was found to directly interact with the N-terminal domain of CLN3. His_6-RILP (~55 kDa) interacts directly with the cytoplasmic loop of CLN3. *Load* represents the percentage of total protein used

significantly less Xpress-Rab7 than the antibody produced against the amino acids 242–258 of the major cytoplasmic loop segment of CLN3 (Online Resource 1). This indicates that the epitopic sites of the polyclonal CLN3 1–33 antibody overlap with the binding region of Rab7. As expected by the GST pull-down experiment, the anti-CLN3 1–33 did not interfere with the co-immunoprecipitation of RILP (Online Resource 1). Since RILP also co-immunoprecipitated with anti-CLN3 242–258 produced against the antigen from the same cytoplasmic loop domain of CLN3 that binds RILP (Fig. 8 and Online Resource 1), the interaction between the two proteins most likely occurs via amino acids outside of the region 242–258 of the cytoplasmic loop of CLN3.

Altogether, these experiments show that CLN3 interacts directly with active, GTP-bound Rab7 and RILP proteins and that these interactions are mediated through different cytoplasmic domains of CLN3.

CLN3 deficiency destabilises GTP-Rab7 on late endocytic compartments

To assess the possible effect of CLN3 deficiency on the GTP/GDP cycle of Rab7, juvenile CLN3 disease and

control fibroblasts were transfected with EGFP-Rab7, and analysed by the fluorescence recovery after photobleaching (FRAP) technique. Perinuclear clusters of EGFP-Rab7 containing endosomes/lysosomes were photobleached at 42-μm^2 area, and the recovery of fluorescence was monitored for 500 s. In the control cells, a recovery curve stabilised close to 60% after 500 s (Fig. 9a). Fibroblasts carrying CLN3E295K and CLN3Δex7-8 mutations in different alleles (compound heterozygous) [38] did not show notable differences in the recovery curve compared to the control cells (Fig. 9a). However, in fibroblasts carrying homozygous CLN3Δex7-8 mutation, which leads to ER retention of the protein, the recovery was markedly faster than measured in the control cells. The homozygous cells already showed ≥50% recovery after 100 s, and reached ≥80% recovery after 500 s. (Fig. 9a). Immunofluorescence images of different time points of recovering cells show that the vesicular pattern of recovering cells resembles the one before the photobleaching (Fig. 9b, shown for control and homozygous CLN3Δex7-8/CLN3Δex7-8 cells). This indicates that the recovery of vesicular EGFP-Rab7 signal reflects recruitment of unbleached cytoplasmic Rab7 on endosomal/lysosomal membranes rather than the movement of unbleached Rab7-positive organelles. Consequently, these results indicate that lysosomes devoid of CLN3 protein display a shorter residence of EGFP-Rab7 on endosomal/lysosomal membranes therefore suggesting unbalanced GTP/GDP cycle of Rab7 in CLN3 deficiency.

Discussion

The function of CLN3 has been studied extensively during the past 15 years with the protein being suggested to participate in a variety of cellular processes, including membrane trafficking in various intracellular compartments [3, 8–19, 21, 24–29, 47]. However, only a few molecular interactions of CLN3, related to the corresponding trafficking steps, have been reported [26, 27] and, therefore, the role of CLN3 in membrane trafficking has remained unclear. CLN3 has been localised to many intracellular compartments (reviewed in [1, 3, 12, 24]) with endosomes and lysosomes being the most prominent sites of putative CLN3 action. This view is also supported by the finding that CLN3 contains well-conserved lysosomal targeting signals recognised by adaptor proteins responsible for protein targeting downstream of the trans-Golgi network [4, 48]. Here, we show that CLN3 interacts directly with active GTP-Rab7 and its effector RILP, and affects the location of the late endosomes/lysosomes possibly through its interactions with microtubular motor protein complexes.

The connection between CLN3 deficiency and disturbances in the steady-state localisation of endosomal/lysosomal compartments has previously been introduced with immortalised neuronal precursor cells prepared from *Cln3Δex7-8* knock-in mouse [3]. Both early and late endosomal compartments were suggested to be more dispersed in *Cln3Δex7-8* cerebellar neurons compared to wild-type controls [3]. In the current study, we report the opposite effect, since over-expression of mutant CLN3E295K in HeLa cells induced perinuclear clustering of late endosomes/lysosomes, with no obvious effect on early endosomal compartments. In addition, analyses of control and juvenile CLN3 disease fibroblasts, carrying either compound heterozygous mutation (CLN3E295K/CLN3Δex7-8) or homozygous mutation (CLN3Δex7-8/CLN3Δex7-8), showed that perinuclear clustering of late endosomal compartments is also evident in patient cells (Online Resource 2). Together with previous data, our results imply that the changes in the vesicular distribution induced by CLN3 mutants may be dependent on the cell type. We show that CLN3 interacts with components of both minus and plus end-directed microtubular motor complexes and that knock-down of CLN3 in HeLa cells affects the outward movement of late endosomes/lysosomes. Combined with the previous reports on the defects in the endocytic pathway of CLN3-deficient cells [3, 27], our data also suggest that CLN3 is involved in bi-directional trafficking of late endosomal compartments and, therefore, has a significant role in the intracellular trafficking system.

We have previously shown that CLN3 binds to the endocytic microtubule-binding protein Hook1 [27]. The yeast ortholog of Hook1, Btn2p, mediates protein sorting between late endosomes and the Golgi complex, in addition to other biological functions ([49] and references therein, [50]). Hook1 may have a more general role in mammalian membrane trafficking since it interacts with several Rab proteins, including Rab7 [27]. We now show that CLN3 also interacts with Rab7, and its effector RILP, although it remains unclear whether the CLN3/Rab7 complex also includes Hook1. Over-expression of CLN3 induces aggregation of Hook1, and thereupon Hook1 cannot be co-immunoprecipitated with CLN3 ([27], and unpublished data). This suggests that Hook1 is not required for the interaction between CLN3 and Rab7, but may instead compete with CLN3 for binding to Rab7.

Rab7 regulates retrograde membrane trafficking downstream of early endosomes and is, to date, the only Rab-family protein shown to regulate the membrane trafficking step between late endosomes and lysosomes [51–54]. This highlights the importance of Rab7 and its effectors in lysosomal functions. So far, several mammalian effectors of Rab7 have been identified, namely Rabring [55], RILP [43], ORP1L [32, 56], FYCO1 [57], Rubicon [58] and potentially Hook1 [27]. RILP binds the $p150^{Glued}$ subunit

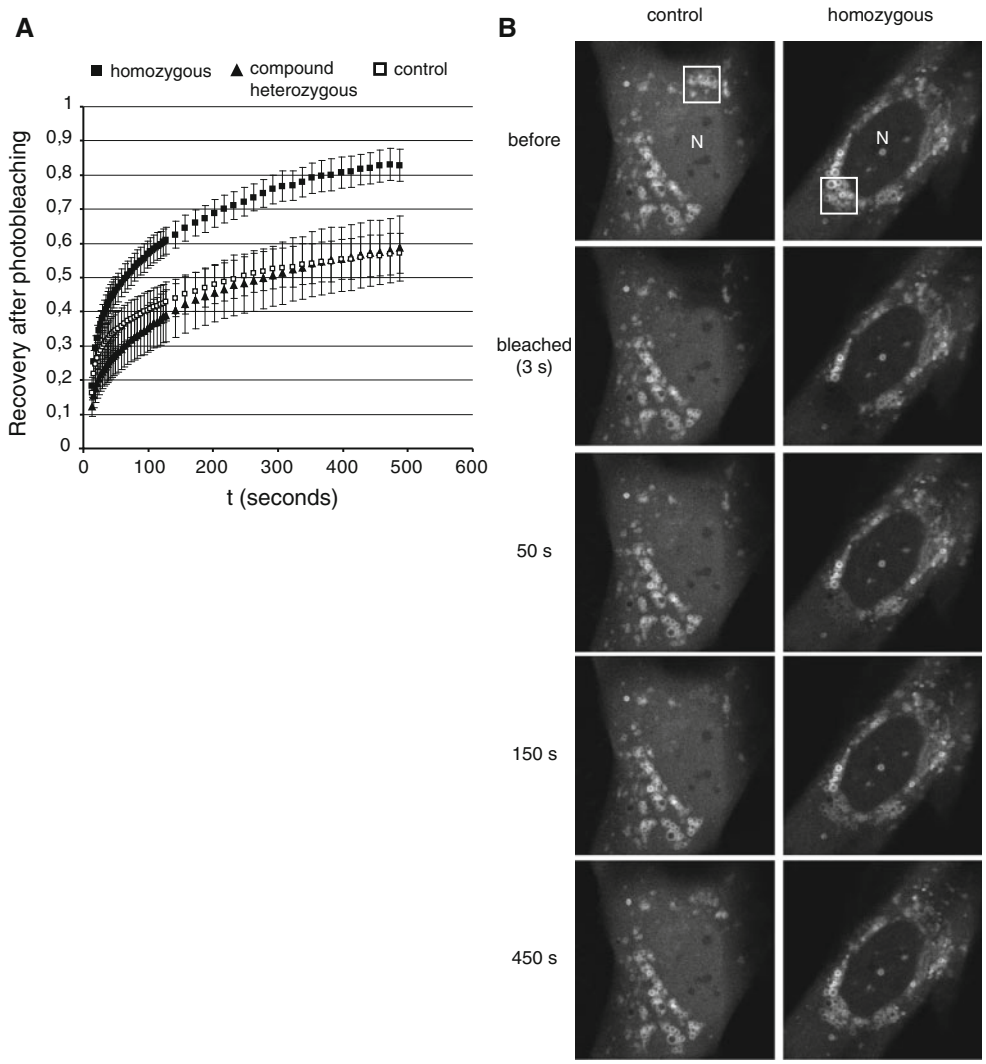

Fig. 9 **a**, **b** Loss of lysosomal CLN3 impairs the GTP/GDP cycle of Rab7. **a** To assess the possible effects of CLN3 deficiency on the GTP/GDP cycle of Rab7, fibroblasts from healthy control and from two juvenile CLN3 disease patients, carrying CLN3Δex7-8/CLN3Δex7-8 (homozygous) or CLN3E295K/CLN3Δex7-8 (compound heterozygous) mutations, were transfected with EGFP-Rab7. The EGFP fluorescence of late endosomal/lysosomal compartments was bleached, and fluorescence recovery (shown relative to the starting value, *y-axis*) as a function of time (*x-axis*) was recorded. CLN3Δex7-8 homozygous cells showed accelerated recovery rates of EGFP-Rab7 signal. Each data point represents mean ± SEM of five recordings from different cells. **b** Immunofluorescence images of different time points of recovering cells (shown for control and homozygous CLN3Δex7-8/CLN3Δex7-8 cells). The bleached area is depicted by a *square*. *N* indicates the nucleus

of the dynactin complex and ORP1L in the same complex translates cholesterol content in late endosomes to interactions with the ER protein VAP-A that controls the binding of $p150^{Glued}$ to its receptor Rab7-RILP and subsequent intracellular positioning of late endosomes ([34] and references therein, [45]). The current data introduce another component, CLN3, that interacts directly with the GTP-bound Rab7 and its effector protein RILP. Based on the GST pull-down and mammalian two-hybrid experiments, the direct interaction between the N-terminal peptide of CLN3 and Rab7 is relatively weak. The interaction between full-length proteins could be stabilised by other CLN3 interacting proteins such as RILP and this dual interaction may increase the avidity of binding to the late endosomal multi-spanning membrane protein CLN3.

Our finding that expression of mutant CLN3E295K increased co-localisation between Rab7 and LAMP-1-positive membranes suggests that late endosomal/lysosomal membrane association of Rab7 was enhanced. The membrane association of Rab proteins is dominated by their nucleotide-bound state [59] and the GTPase-deficient constitutively active Rab7Q67L mutant has been shown to be more efficiently distributed to lysosomal compartments [60]. We show that CLN3 preferably binds GTP-bound

Rab7 and suggest that expression of CLN3E295K affects Rab7 function on endosomal/lysosomal compartments. Patients harbouring the CLN3E295K mutation are compound heterozygous (CLN3E295K/CLN3Δex7-8) and display a protracted disease phenotype [38]. Therefore, the CLN3E295K mutant likely possesses endosomal/lysosomal function(s) which in vivo do not result in an acute, severe insult on Rab7, but rather abnormaltities which become lethal over time. These changes most likely result from disturbances in the interactions between CLN3E295K, RILP and Rab7 proteins (Online Resource 3c, d). Here, and in the previous works, CLN3 as well as its interacting partners dynactin, Rab7 and RILP, have all been linked to both dynein- and kinesin-dependent membrane trafficking. These findings, together with the possibility that CLN3 deficiency affects in a cell type-specific manner the localisation of endosomal/lysosomal compartments, impede us, at the moment, from concluding in more detail how disturbances in the CLN3 interactions caused by E295K mutation could affect membrane trafficking. The loss of lysosomal CLN3, however, could have a major effect on the function of Rab7. This is supported by the observation that juvenile CLN3 disease fibroblasts, with no lysosomal CLN3 (CLN3Δex7-8 homozygous), display an unbalanced Rab7 GTP/GDP cycle which is most likely due to the fact that the deletion of exons 7–8 in CLN3 results in a truncated protein lacking the determined RILP-binding domain, and, more importantly, is retained in the ER where it is incapable of interacting with the late endosomal/lysosomal Rab7 and RILP proteins. We demonstrated this experimentally in the case of Rab7 (Online Resource 3a, b).

Rab7 has been shown to mediate axonal retrograde trafficking of neurotrophins [61, 62], and mutations in Rab7 result in neurodegenerative conditions [63]. Furthermore, many abnormalities observed in CLN3 deficiency are closely associated with the function of Rab7. CLN3 deficiency affects lysosomal/vacuolar pH and size [3, 12, 14, 15, 18], processing of lysosomal hydrolases [3, 13, 25] and autophagy [8, 64]. These processes are interconnected and all have previously been shown to be affected by dysfunctional Rab7 [51, 65–68]. Interestingly, both CLN3 and Rab7 are localised in autophagosomal membranes and suggested to have a role in maturation of late autophagic vesicles [8, 67]. Thus, impairment of the Rab7-mediated intracellular trafficking could have a significant role in pathogenesis of CLN3 disease causing defects in neuronal endocytic trafficking and autophagic processes, which ultimately may result in neurodegeneration.

Acknowledgments Auli Toivola, Seija Puomilahti, Anne Nyberg, and Kathrin Oelgeschläger are thanked for excellent technical assistance. We thank the Biomedicum Imaging Unit (Biomedicum, Helsinki, Finland) for providing the facilities for the image analysis. This work was supported by the Academy of Finland, Centre of Excellence in Complex Disease Genetics [129680], the Sigrid Juselius Foundation, Rinnekoti Research Foundation/Brain Foundation of Finland and the Finnish Cultural Foundation.

References

1. Phillips SN, Benedict JW, Weimer JM, Pearce DA (2005) CLN3, the protein associated with batten disease: structure, function and localization. J Neurosci Res 79(5):573–583
2. Jarvela I, Lehtovirta M, Tikkanen R, Kyttala A, Jalanko A (1999) Defective intracellular transport of CLN3 is the molecular basis of Batten disease (JNCL). Hum Mol Genet 8(6):1091–1098
3. Fossale E, Wolf P, Espinola JA, Lubicz-Nawrocka T, Teed AM, Gao H, Rigamonti D, Cattaneo E, Macdonald ME, Cotman SL (2004) Membrane trafficking and mitochondrial abnormalities precede subunit c deposition in a cerebellar cell model of juvenile neuronal ceroid lipofuscinosis. BMC Neurosci 5(1):57
4. Kyttala A, Ihrke G, Vesa J, Schell MJ, Luzio JP (2004) Two motifs target Batten disease protein CLN3 to lysosomes in transfected nonneuronal and neuronal cells. Mol Biol Cell 15(3):1313–1323
5. Luiro K, Kopra O, Lehtovirta M, Jalanko A (2001) CLN3 protein is targeted to neuronal synapses but excluded from synaptic vesicles: new clues to Batten disease. Hum Mol Genet 10(19):2123–2131
6. Consortium (1995) Isolation of a novel gene underlying Batten disease, CLN3. The International Batten Disease Consortium. Cell 82(6):949–957
7. Haltia M (2006) The neuronal ceroid-lipofuscinoses: from past to present. Biochim Biophys Acta 1762(10):850–856
8. Cao Y, Espinola JA, Fossale E, Massey AC, Cuervo AM, MacDonald ME, Cotman SL (2006) Autophagy is disrupted in a knock-in mouse model of juvenile neuronal ceroid lipofuscinosis. J Biol Chem 281(29):20483–20493
9. Hobert JA, Dawson G (2007) A novel role of the Batten disease gene CLN3: association with BMP synthesis. Biochem Biophys Res Commun 358(1):111–116
10. Lane SC, Jolly RD, Schmechel DE, Alroy J, Boustany RM (1996) Apoptosis as the mechanism of neurodegeneration in Batten's disease. J Neurochem 67(2):677–683
11. Narayan SB, Rakheja D, Tan L, Pastor JV, Bennett MJ (2006) CLN3P, the Batten's disease protein, is a novel palmitoyl-protein Delta-9 desaturase. Ann Neurol 60(5):570–577
12. Gachet Y, Codlin S, Hyams JS, Mole SE (2005) btn1, the Schizosaccharomyces pombe homologue of the human Batten disease gene CLN3, regulates vacuole homeostasis. J Cell Sci 118(Pt 23):5525–5536
13. Golabek AA, Kida E, Walus M, Kaczmarski W, Michalewski M, Wisniewski KE (2000) CLN3 protein regulates lysosomal pH and alters intracellular processing of Alzheimer's amyloid-beta protein precursor and cathepsin D in human cells. Mol Genet Metab 70(3):203–213
14. Holopainen JM, Saarikoski J, Kinnunen PK, Jarvela I (2001) Elevated lysosomal pH in neuronal ceroid lipofuscinoses (NCLs). Eur J Biochem 268(22):5851–5856
15. Pearce DA, Ferea T, Nosel SA, Das B, Sherman F (1999) Action of BTN1, the yeast orthologue of the gene mutated in Batten disease. Nat Genet 22(1):55–58
16. Kim Y, Ramirez-Montealegre D, Pearce DA (2003) A role in vacuolar arginine transport for yeast Btn1p and for human CLN3,

the protein defective in Batten disease. Proc Natl Acad Sci USA 100(26):15458–15462
17. Ramirez-Montealegre D, Pearce DA (2005) Defective lysosomal arginine transport in juvenile Batten disease. Hum Mol Genet 14(23):3759–3773
18. Kitzmuller C, Haines RL, Codlin S, Cutler DF, Mole SE (2008) A function retained by the common mutant CLN3 protein is responsible for the late onset of juvenile neuronal ceroid lipofuscinosis. Hum Mol Genet 17(2):303–312
19. Tuxworth RI, Vivancos V, O'Hare MB, Tear G (2009) Interactions between the juvenile Batten disease gene, CLN3, and the Notch and JNK signalling pathways. Hum Mol Genet 18(4):667–678
20. Tuxworth RI, Chen H, Vivancos V, Carvajal N, Huang X, Tear G (2011) The Batten disease gene CLN3 is required for the response to oxidative stress. Hum Mol Genet 20(10):2037–2047
21. Chang JW, Choi H, Kim HJ, Jo DG, Jeon YJ, Noh JY, Park WJ, Jung YK (2007) Neuronal vulnerability of CLN3 deletion to calcium-induced cytotoxicity is mediated by calsenilin. Hum Mol Genet 16(3):317–326
22. Vitiello SP, Benedict JW, Padilla-Lopez S, Pearce DA (2010) Interaction between Sdo1p and Btn1p in the Saccharomyces cerevisiae model for Batten disease. Hum Mol Genet 19(5): 931–942
23. Getty AL, Benedict JW, Pearce DA (2011) A novel interaction of CLN3 with nonmuscle myosin-IIB and defects in cell motility of Cln3(−/−) cells. Exp Cell Res 317(1):51–69
24. Codlin S, Mole SE (2009) S. pombe btn1, the orthologue of the Batten disease gene CLN3, is required for vacuole protein sorting of Cpy1p and Golgi exit of Vps10p. J Cell Sci 122(Pt 8): 1163–1173
25. Metcalf DJ, Calvi AA, Seaman M, Mitchison HM, Cutler DF (2008) Loss of the Batten disease gene CLN3 prevents exit from the TGN of the mannose 6-phosphate receptor. Traffic (Copenhagen, Denmark) 9(11):1905–1914
26. Uusi-Rauva K, Luiro K, Tanhuanpaa K, Kopra O, Martin-Vasallo P, Kyttala A, Jalanko A (2008) Novel interactions of CLN3 protein link Batten disease to dysregulation of fodrin-Na^+, K^+ ATPase complex. Exp Cell Res 314(15):2895–2905
27. Luiro K, Yliannala K, Ahtiainen L, Maunu H, Jarvela I, Kyttala A, Jalanko A (2004) Interconnections of CLN3, Hook1 and Rab proteins link Batten disease to defects in the endocytic pathway. Hum Mol Genet 13(23):3017–3027
28. Weimer JM, Custer AW, Benedict JW, Alexander NA, Kingsley E, Federoff HJ, Cooper JD, Pearce DA (2006) Visual deficits in a mouse model of Batten disease are the result of optic nerve degeneration and loss of dorsal lateral geniculate thalamic neurons. Neurobiol Dis 22(2):284–293
29. Luiro K, Kopra O, Blom T, Gentile M, Mitchison HM, Hovatta I, Tornquist K, Jalanko A (2006) Batten disease (JNCL) is linked to disturbances in mitochondrial, cytoskeletal, and synaptic compartments. J Neurosci Res 84(5):1124–1138
30. Cai T, Wang H, Chen Y, Liu L, Gunning WT, Quintas LE, Xie ZJ (2008) Regulation of caveolin-1 membrane trafficking by the Na/K-ATPase. J Cell Biol 182(6):1153–1169
31. Jarvela I, Sainio M, Rantamaki T, Olkkonen VM, Carpen O, Peltonen L, Jalanko A (1998) Biosynthesis and intracellular targeting of the CLN3 protein defective in Batten disease. Hum Mol Genet 7(1):85–90
32. Johansson M, Olkkonen VM (2005) Assays for interaction between Rab7 and oxysterol binding protein related protein 1L (ORP1L). Methods Enzymol 403:743–758
33. Marsman M, Jordens I, Kuijl C, Janssen L, Neefjes J (2004) Dynein-mediated vesicle transport controls intracellular Salmonella replication. Mol Biol Cell 15(6):2954–2964
34. Johansson M, Rocha N, Zwart W, Jordens I, Janssen L, Kuijl C, Olkkonen VM, Neefjes J (2007) Activation of endosomal dynein motors by stepwise assembly of Rab7-RILP-p150Glued, ORP1L, and the receptor betalll spectrin. J Cell Biol 176(4):459–471
35. Jordens I, Fernandez-Borja M, Marsman M, Dusseljee S, Janssen L, Calafat J, Janssen H, Wubbolts R, Neefjes J (2001) The Rab7 effector protein RILP controls lysosomal transport by inducing the recruitment of dynein-dynactin motors. Curr Biol 11(21): 1680–1685
36. Heuser J (1989) Changes in lysosome shape and distribution correlated with changes in cytoplasmic pH. J Cell Biol 108(3):855–864
37. Brown CL, Maier KC, Stauber T, Ginkel LM, Wordeman L, Vernos I, Schroer TA (2005) Kinesin-2 is a motor for late endosomes and lysosomes. Traffic (Copenhagen, Denmark) 6(12): 1114–1124
38. Aberg L, Lauronen L, Hamalainen J, Mole SE, Autti T (2009) A 30-year follow-up of a neuronal ceroid lipofuscinosis patient with mutations in CLN3 and protracted disease course. Pediatr Neurol 40(2):134–137
39. Echeverri CJ, Paschal BM, Vaughan KT, Vallee RB (1996) Molecular characterization of the 50-kD subunit of dynactin reveals function for the complex in chromosome alignment and spindle organization during mitosis. J Cell Biol 132(4):617–633
40. Nakata T, Hirokawa N (1995) Point mutation of adenosine triphosphate-binding motif generated rigor kinesin that selectively blocks anterograde lysosome membrane transport. J Cell Biol 131(4):1039–1053
41. Tanaka Y, Kanai Y, Okada Y, Nonaka S, Takeda S, Harada A, Hirokawa N (1998) Targeted disruption of mouse conventional kinesin heavy chain, kif5B, results in abnormal perinuclear clustering of mitochondria. Cell 93(7):1147–1158
42. Wubbolts R, Fernandez-Borja M, Jordens I, Reits E, Dusseljee S, Echeverri C, Vallee RB, Neefjes J (1999) Opposing motor activities of dynein and kinesin determine retention and transport of MHC class II-containing compartments. J Cell Sci 112(Pt 6):785–795
43. Cantalupo G, Alifano P, Roberti V, Bruni CB, Bucci C (2001) Rab-interacting lysosomal protein (RILP): the Rab7 effector required for transport to lysosomes. EMBO J 20(4):683–693
44. Wu M, Wang T, Loh E, Hong W, Song H (2005) Structural basis for recruitment of RILP by small GTPase Rab7. EMBO J 24(8):1491–1501
45. Rocha N, Kuijl C, van der Kant R, Janssen L, Houben D, Janssen H, Zwart W, Neefjes J (2009) Cholesterol sensor ORP1L contacts the ER protein VAP to control Rab7-RILP-p150 Glued and late endosome positioning. J Cell Biol 185(7):1209–1225
46. Leung KY, Greene ND, Munroe PB, Mole SE (2001) Identification of a transactivation motif in the CLN3 protein. IUBMB Life 51(5):295–298
47. Getty AL, Benedict JW, Pearce DA (2011) A novel interaction of CLN3 with nonmuscle myosin-IIB and defects in cell motility of Cln3(−/−) cells. Exp Cell Res 317(1):51–69
48. Kyttala A, Yliannala K, Schu P, Jalanko A, Luzio JP (2005) AP-1 and AP-3 facilitate lysosomal targeting of Batten disease protein CLN3 via its dileucine motif. J Biol Chem 280(11):10277–10283
49. Kim Y, Chattopadhyay S, Locke S, Pearce DA (2005) Interaction among Btn1p, Btn2p, and Ist2p reveals potential interplay among the vacuole, amino acid levels, and ion homeostasis in the yeast *Saccharomyces cerevisiae*. Eukaryot Cell 4(2):281–288
50. Kama R, Robinson M, Gerst JE (2007) Btn2, a Hook1 ortholog and potential Batten disease-related protein, mediates late endosome-Golgi protein sorting in yeast. Mol Cell Biol 27(2):605–621
51. Bucci C, Thomsen P, Nicoziani P, McCarthy J, van Deurs B (2000) Rab7: a key to lysosome biogenesis. Mol Biol Cell 11(2):467–480
52. Feng Y, Press B, Wandinger-Ness A (1995) Rab 7: an important regulator of late endocytic membrane traffic. J Cell Biol 131(6 Pt 1):1435–1452

53. Vanlandingham PA, Ceresa BP (2009) Rab7 regulates late endocytic trafficking downstream of multivesicular body biogenesis and cargo sequestration. J Biol Chem 284(18):12110–12124
54. Vitelli R, Santillo M, Lattero D, Chiariello M, Bifulco M, Bruni CB, Bucci C (1997) Role of the small GTPase Rab7 in the late endocytic pathway. J Biol Chem 272(7):4391–4397
55. Mizuno K, Kitamura A, Sasaki T (2003) Rabring7, a novel Rab7 target protein with a RING finger motif. Mol Biol Cell 14(9): 3741–3752
56. Johansson M, Lehto M, Tanhuanpaa K, Cover TL, Olkkonen VM (2005) The oxysterol-binding protein homologue ORP1L interacts with Rab7 and alters functional properties of late endocytic compartments. Mol Biol Cell 16(12):5480–5492
57. Pankiv S, Alemu EA, Brech A, Bruun JA, Lamark T, Overvatn A, Bjorkoy G, Johansen T (2010) FYCO1 is a Rab7 effector that binds to LC3 and PI3P to mediate microtubule plus end-directed vesicle transport. J Cell Biol 188(2):253–269
58. Sun Q, Westphal W, Wong KN, Tan I, Zhong Q (2010) Rubicon controls endosome maturation as a Rab7 effector. Proc Natl Acad Sci USA 107(45):19338–19343
59. Stein MP, Dong J, Wandinger-Ness A (2003) Rab proteins and endocytic trafficking: potential targets for therapeutic intervention. Adv Drug Deliv Rev 55(11):1421–1437
60. Meresse S, Gorvel JP, Chavrier P (1995) The rab7 GTPase resides on a vesicular compartment connected to lysosomes. J Cell Sci 108(Pt 11):3349–3358
61. Deinhardt K, Salinas S, Verastegui C, Watson R, Worth D, Hanrahan S, Bucci C, Schiavo G (2006) Rab5 and Rab7 control endocytic sorting along the axonal retrograde transport pathway. Neuron 52(2):293–305
62. Saxena S, Bucci C, Weis J, Kruttgen A (2005) The small GTPase Rab7 controls the endosomal trafficking and neuritogenic signaling of the nerve growth factor receptor TrkA. J Neurosci 25(47):10930–10940
63. Verhoeven K, De Jonghe P, Coen K, Verpoorten N, Auer-Grumbach M, Kwon JM, FitzPatrick D, Schmedding E, De Vriendt E, Jacobs A, Van Gerwen V, Wagner K, Hartung HP, Timmerman V (2003) Mutations in the small GTP-ase late endosomal protein RAB7 cause Charcot-Marie-Tooth type 2B neuropathy. Am J Hum Genet 72(3):722–727
64. Song JW, Misgeld T, Kang H, Knecht S, Lu J, Cao Y, Cotman SL, Bishop DL, Lichtman JW (2008) Lysosomal activity associated with developmental axon pruning. J Neurosci 28(36): 8993–9001
65. Braulke T, Geuze HJ, Slot JW, Hasilik A, von Figura K (1987) On the effects of weak bases and monensin on sorting and processing of lysosomal enzymes in human cells. Eur J Cell Biol 43(3):316–321
66. Gutierrez MG, Munafo DB, Beron W, Colombo MI (2004) Rab7 is required for the normal progression of the autophagic pathway in mammalian cells. J Cell Sci 117(Pt 13):2687–2697
67. Jager S, Bucci C, Tanida I, Ueno T, Kominami E, Saftig P, Eskelinen EL (2004) Role for Rab7 in maturation of late autophagic vacuoles. J Cell Sci 117(Pt 20):4837–4848
68. Press B, Feng Y, Hoflack B, Wandinger-Ness A (1998) Mutant Rab7 causes the accumulation of cathepsin D and cation-independent mannose 6-phosphate receptor in an early endocytic compartment. J Cell Biol 140(5):1075–1089